Hyperplasia of Lymphatic Vessels in VEGF-C Transgenic Mice

Michael Jeltsch,* Arja Kaipainen,* Vladimir Joukov, Xiaojuan Meng, Merja Lakso, Heikki Rauvala, Melody Swartz, Dai Fukumura, Rakesh K. Jain, Kari Alitalo†

No growth factors specific for the lymphatic vascular system have yet been described. Vascular endothelial growth factor (VEGF) regulates vascular permeability and angiogenesis, but does not promote lymphangiogenesis. Overexpression of VEGF-C, a ligand of the VEGF receptors VEGFR-3 and VEGFR-2, in the skin of transgenic mice resulted in lymphatic, but not vascular, endothelial proliferation and vessel enlargement. Thus, VEGF-C induces selective hyperplasia of the lymphatic vasculature, which is involved in the draining of interstitial fluid and in immune function, inflammation, and tumor metastasis. VEGF-C may play a role in disorders involving the lymphatic system and may be of potential use in therapeutic lymphangiogenesis.

The four known members of the VEGF family, VEGF (*1*), VEGF-B (*2*), VEGF-C (*3*, *4*), and platelet-derived growth factor (*5*) have different roles as regulatory factors of endothelia (*6*). In order to clarify the function of VEGF-C in vivo, its cDNA was cloned between the human keratin 14 (K14) promoter and polyadenylation signal for expression in transgenic mice (*7*). The K14 promoter has been shown to target gene expression to the basal cells of stratified squamous epithelia (*8*). Of the 27 mice analyzed at 3 weeks of age, three were transgene-positive, having approximately 40 to 50, 20, and 4 to 6 copies, respectively, of the transgene in their genome. The latter two mice transmitted the gene to two of 40 and six of 11 pups, respectively.

The transgenic mice were small and had slightly swollen eyelids and poorly developed fur. Histological examination showed that the epidermis was hyperplastic and the number of hair follicles was reduced; these effects were considered secondary to other phenotypic changes (*9*). The dermis was atrophic, and its connective tissue was replaced by large, dilated vessels devoid of red cells but lined with a thin endothelial cell layer (Fig. 1, A and B). Such abnormal vessels were confined to the dermis and resembled the dysfunctional, dilated spaces characteristic of hyperplastic lymphatic vessels (*10*). In addition, the ultrastructural features were reminiscent of lymphatic vessels, which differ from blood vessels in that they have overlapping endothelial junctions, anchoring filaments in the vessel wall, and a discontinuous or even partially absent basement membrane (Fig. 1C) (*11*). Antibodies to collagen types IV and XVIII (*12*), and laminin gave little or no staining of the vessels, whereas the basement membrane staining of other vessels was prominent (Fig. 1D) (*13*). The endothelium was also characterized by positive staining with monoclonal antibodies to desmoplakins I and II, expressed in lymphatic, but not in vascular endothelial cells (*14*). Collectively, these findings suggest that the abnormal vessels are of lymphatic origin.

Abundant VEGF-C mRNA was detected in the epidermis and hair follicles of the transgenic mice (Fig. 2, A and B), whereas mRNAs encoding its receptors VEGFR-3 (*15*) and VEGFR-2 (*16*), as well as the Tie-1 endothelial receptor tyrosine kinase (*17*), were expressed in endothelial cells lining the abnormal vessels (Fig. 2, C and E) (*13*). In the skin of littermate control animals, VEGFR-3 was detected only in the superficial subpapillary layer of lymphatic vessels, whereas VEGFR-2 was observed in all endothelia (Fig. 2, D and F), in agreement with earlier findings (*18*, *19*).

The lymphatic endothelium has a great capacity to distend in order to adapt to functional requirements. To ascertain whether vessel dilation was due to endothelial distension or proliferation, we carried out in vitro proliferation assays. The VEGF-C receptor interaction in the transgenic mice apparently transduces a mitogenic signal, because in contrast to littermate controls, the lymphatic endothelium of the skin from young K14–VEGF-C mice showed increased DNA synthesis, as demonstrated by bromodeoxyuridine (BrdU) incorporation followed by staining with antibodies to BrdU (Fig. 3, A and B).

Angiogenesis is a multistep process that includes endothelial sprouting, migration, and proliferation (*20*). To estimate the contribution of such processes to the transgenic phenotype, we analyzed the morphology and function of the lymphatic vessels, using fluorescent microlymphography (*21*). A typical honeycomb-like network with similar mesh sizes was detected in both control and transgenic mice (Fig. 3, C and D), but the diameter of the vessels in transgenic

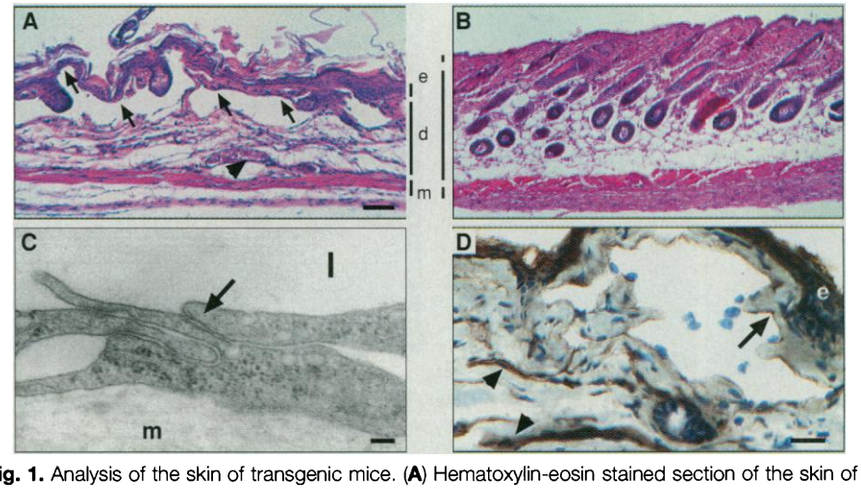

Fig. 1. Analysis of the skin of transgenic mice. (**A**) Hematoxylin-eosin stained section of the skin of a 2-month-old transgenic mouse. Hyperkeratotic epidermis (e) showed underlying vessel spaces lined with endothelium (arrows) but devoid of red cells (compare with the dermal vein shown with an arrowhead). The dermis (d) is atrophic compared with the control littermate skin (**B**) (45% versus 65% of the dermal thickness, respectively), and the muscle layer (m) is also reduced. (**C**) Electron microscopy shows the endothelial junctions of an abnormal vessel (arrow) (*25*); l, lumen; m, mesenchyme. In (**D**), the basal lamina is stained for type XVIII collagen in veins (arrowheads) but not in the lymphatic endothelium (arrow) (*26*). Scale bars for (A) and (B), 250 μm; (C), 100 nm; and (D), 25 μm.

M. Jeltsch, A. Kaipainen, V. Joukov, K. Alitalo, Molecular/Cancer Biology Laboratory, Haartman Institute, Post Office Box 21 (Haartmaninkatu 3), University of Helsinki, SF-00014 Helsinki, Finland.
X. Meng, M. Lakso, H. Rauvala, Biotechnology Institute, 00014 University of Helsinki, Helsinki, Finland.
M. Swartz, D. Fukumura, R. K. Jain, Department of Radiation Oncology, Massachusetts General Hospital and Harvard Medical School, Boston, MA 02114, USA.

*These authors contributed equally to this work.
†To whom correspondence should be addressed. E-mail: Kari.Alitalo@Helsinki.FI

mice was approximately twice that of controls (Table 1). Some dysfunction of the abnormal vessels was indicated by the fact that it took longer for the dextran to completely fill the abnormal vessels. Injection of fluorescein isothiocyanate (FITC)–dextran into the tail vein, followed by fluorescence microscopy of the ear showed that the blood vascular morphology was unaltered and leukocyte rolling and adherence appeared normal (Fig. 3, E and F) (*13*). Thus, the endothelial proliferation induced by VEGF-C leads to hyperplasia of the superficial lymphatic network, but does not induce the sprouting of new vessels.

These effects of VEGF-C overexpression are unexpectedly specific, particularly as VEGF-C is also capable of binding to and activating VEGFR-2, which is the major mitogenic receptor of blood vessel endothelial cells (*16*). In culture, high concentrations of VEGF-C stimulate the growth and migration of bovine capillary endothelial cells that express VEGFR-2, but not significant amounts of VEGFR-3 (*3*). In addition, VEGF-C induces vascular permeability in the Miles assay, presumably by its effect on VEGFR-2 (*22*). In vivo, the specific effects of VEGF-C on lymphatic endothelial cells may reflect a requirement for the formation of VEGFR-3 × VEGFR-2 heterodimers for endothelial cell proliferation at physiological concentrations of the growth factor. Such possible heterodimers may help to explain how three homologous VEGFs exert partially redundant, yet strikingly specific, biological effects.

In summary, VEGF-C appears to induce specific lymphatic endothelial proliferation and hyperplasia of the lymphatic vascula-

Table 1. Structural parameters of lymphatic and blood vessel networks for transgenic and control mice. Mesh size describes vessel density. Diameters and mesh sizes are in micrometers (mean ± SD).

Parameter	Transgenic	Control	*P* value*
	Lymphatic vessels†		
Diameter	142.3 ± 26.2	68.2 ± 21.7	0.0143
Horizontal mesh size	1003 ± 87.1	960.8 ± 93.1	0.2207
Vertical mesh size	507.3 ± 58.9	488.8 ± 59.9	0.5403
	Blood vessels‡		
Median diameter	8.3 ± 0.6	7.6 ± 1.1	0.1213
Vessel density (cm/cm^2)	199.2 ± 6.6	216.4 ± 20.0	0.3017

*Mann-Whitney test. †Number of animals for transgenic and control groups were 4 and 5, respectively. ‡Number of animals for transgenic and control groups were 3 and 6, respectively.

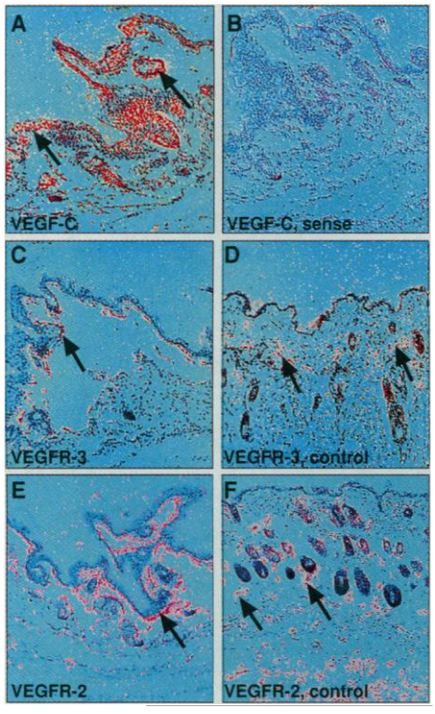

Fig. 2. In situ hybridization analysis of the skin of K14–VEGF-C transgenic mice. (**A**) and (**B**) show hybridization of transgenic skin with VEGF-C antisense and sense probes. (**C**) and (**D**) and (**E**) and (**F**) show in situ hybridization for VEGFR-3 and VEGFR-2, respectively, in the skin of transgenic and littermate control animals (*27*). Arrows in (A) indicate basal keratinocytes; in (C) through (E), they point out the lymphatic endothelium; and in (F), arrows show endothelial cells. Scale bar, 20 μm.

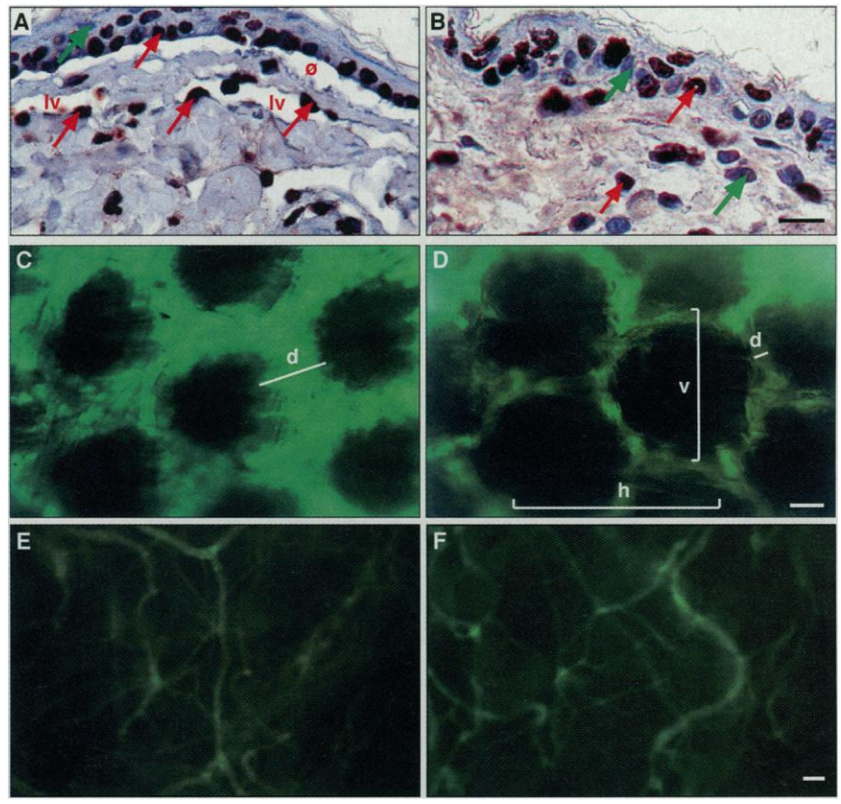

Fig. 3. Immunohistochemical analysis of endothelial proliferation and intravital fluorescence microlymphography and microvessel angiography. (**A**) and (**B**) show staining of cells in the S phase of the cell cycle, through BrdU incorporation into DNA and its immunohistochemical detection (*28*). In 2-week-old transgenic mice, the nuclear staining was observed in many endothelial cells of the lymphatic vessels (lv) as well as in keratinocytes [red arrows in (A)]. In nontransgenic littermates, mainly nuclei of keratinocytes of epidermis and some dermal cells are stained [red arrows in (B)]; unstained nuclei were observed in both cases (green arrows). Ø marks artefactual detachment of the epidermis during sample preparation. (**C**) and (**D**) illustrate the lymphatic vessels of transgenic and control skin, respectively, through fluorescence microscopy after intradermal injection of FITC-dextran (*21, 29*). The measured parameters are diameter (d) [in (C) and (D)] and horizontal (h) and vertical (v) mesh sizes [in (D) only]. Blood vessels of the ear after injection of FITC-dextran into the tail vein of transgenic and control mice are shown in (**E**) and (**F**), respectively (*24*). Scale bars for (A) and (B), 5 μm; (C) and (D), 250 μm; (E) and (F), 1 mm.

ture in vivo. So far, there is no evidence that tumors can stimulate the growth of new lymphatic vessels (*23*), but further studies should establish the role of VEGF-C in lymphangiomas and in tumor metastasis via the lymphatic vasculature as well as in various other disorders involving the lymphatic system and their treatment.

REFERENCES AND NOTES

1. N. Ferrara and T. Davis-Smyth, *Endocr. Rev.*, in press.
2. B. Olofsson *et al.*, *Proc. Natl. Acad. Sci. U.S.A.* **93**, 2576 (1996); S. Grimmond *et al.*, *Genome Res.* **6**, 124 (1996).
3. V. Joukov *et al.*, *EMBO J.* **15**, 290 (1996); J. Lee *et al.*, *Proc. Natl. Acad. Sci. U.S.A.* **93**, 1988 (1996).
4. E. Kukk *et al.*, *Development* **122**, 3829 (1996).
5. D. Maglione, V. Guerriero, G. Viglietto, P. Delli-Bovi, M. G. Persico, *Proc. Natl. Acad. Sci. U.S.A.* **88**, 9267 (1991).
6. M. Klagsbrun and P. A. D'Amore, *Cytokine Growth Factor Rev.* **7**, 259 (1996).
7. The human VEGF-C cDNA (GenBank accession number X94216) was blunt-end ligated to the Bam HI restriction site of the K14 expression cassette (*8*), and an Eco RI–Hind III fragment containing the K14 promoter, VEGF-C cDNA, and K14 polyadenylation signal was isolated and injected into fertilized oocytes of the FVB/NIH strain of mice. The injected zygotes were transplanted into oviducts of pseudopregnant C57BL/6 × DBA/2J hybrid mice. We analyzed the resulting founder mice for the presence of the transgene by polymerase chain reaction of tail DNA, with the primers: 5′-CATGTACGAACCGCCAG-3′ and 5′-AATGACCAGAGAGAGGCGAG-3′. The tail DNAs were also subjected to endonuclease digestion, Southern blotting, and hybridization analysis using the transgene fragment as the probe.
8. R. Vassar, M. Rosenberg, S. Ross, A. Tyner, E. Fuchs, *Proc. Natl. Acad. Sci. U.S.A.* **86**, 1563 (1989).
9. H. J. Leu and J. T. Lie, in *Vascular Pathology* (Chapman & Hall, London, 1995), p. 509.
10. T. W. Fossum and M. W. Miller, *J. Vet. Intern. Med.* **6**, 283 (1992).
11. L. V. Leak, *Microvasc. Res.* **2**, 361 (1970).
12. Y. Muragaki *et al.*, *Proc. Natl. Acad. Sci. U.S.A.* **92**, 8763 (1995); M. Rehn and T. Pihlajaniemi, *ibid.* **91**, 4234 (1994).
13. M. Jeltsch *et al.*, data not shown.
14. M. Schmelz, R. Moll, C. Kuhn, W. W. Franke, *Differentiation* **57**, 97 (1994).
15. K. Pajusola *et al.*, *Cancer Res.* **52**, 5738 (1992); F. Galland *et al.*, *Oncogene* **8**, 1233 (1993).
16. B. I. Terman *et al.*, *Biochem. Biophys. Res. Commun.* **187**, 1579 (1992); B. Millauer *et al.*, *Cell* **72**, 83 (1993).
17. J. Korhonen, A. Polvi, J. Partanen, K. Alitalo, *Oncogene* **9**, 395 (1994).
18. A. Kaipainen *et al.*, *Proc. Natl. Acad. Sci. U.S.A.* **92**, 3566 (1995).
19. T. Yamaguchi, D. Dumont, R. Conion, M. Breitman, J. Rossant, *Development* **118**, 489 (1993); D. Dumont *et al.*, *Dev. Dyn.* **203**, 80 (1995).
20. J. Folkman and Y. J. Shing, *J. Biol. Chem.* **267**, 10931 (1992).
21. A. J. Leu, D. A. Berk, F. Yuan, R. K. Jain, *Am. J. Physiol.* **267**, 1507 (1994); M. A. Swartz, D. A. Berk, R. K. Jain, *ibid.* **270**, 324 (1996).
22. V. Joukov, unpublished data.
23. J. Folkman, *N. Engl. J. Med.* **334**, 921 (1996).
24. D. Fukumura *et al.*, *Cancer Res.* **55**, 4824 (1995).
25. For electron microscopy, tissue pieces from two transgenic skin biopsies were fixed in formaldehyde, postfixed in 2% osmium tetroxide, and embedded in LX 112. Sagittal ultrathin sections were studied with the Jeol1200EX electron microscope.
26. For immunohistochemistry, we stained cryostat sections of 5 to 10 μm from abdominal and back skin with anti-mouse desmoplakin I and II monoclonal antibodies (Progen), affinity-purified rabbit anti-mouse collagen XVIII IgG (a gift from T. Pihlajaniemi), and rabbit anti-mouse laminin IgG (provided by E. Lehtonen), by using the Vectastain ABC Elite kit (Vector Laboratories). Normal mouse or rabbit sera were used as negative controls for the stainings.
27. In situ hybridization of sections was performed as described [A. Kaipainen *et al.*, *J. Exp. Med.* **178**, 2077 (1993)]. The human VEGF-C antisense RNA probe was generated from linearized pCR™II plasmid (Invitrogen) containing an Eco RI fragment corresponding to nucleotides 628 through 1037 of human VEGF-C cDNA. The VEGFR-3 probe was described earlier (*18*). The VEGFR-2 probe was an Eco RI fragment covering base pairs 1958 through 2683 (GenBank accession number X59397, a gift from J. Rossant).
28. For measurement of DNA synthesis, small (3 mm by 3 mm) skin biopsies from four transgenic and four control mice were incubated in Dulbecco's modification of Eagle's medium with 10 μg/ml BrdU for 6 hours at 37°C, fixed in 70% ethanol for 12 hours, and embedded in paraffin. After a 30-min treatment with 0.1% pepsin in 0.1 M HCl at room temperature to denature DNA, staining was carried out as above with mouse monoclonal antibodies to BrdU (Amersham).
29. Fluorescence microlymphography was performed as follows. The staining of the lymphatic network in vivo was carried out as described (*20*). Briefly, 8-week-old mice were anesthetized and placed on a heating pad to maintain a 37°C temperature. A 30-gauge needle, connected to a catheter filled with a solution of FITC-dextran (2 M, 8 mg/ml in phosphate-buffered solution), was injected intradermally into the tip of the tail. The solution was infused with a constant hydrostatic pressure equivalent to a 50-cm column of water (flow rate averaging roughly 0.01 μl/min) until the extent of network filling remained constant (approximately 2 hours). Flow rate and fluorescence intensity were monitored continuously throughout the experiment. The intravital fluorescence microscopy of blood vessels was as described (*24*).

30. We thank E. Saksela for help with histological interpretation; E. Lehtonen for help in electron microscopy; E. Hatva for critical reading of the manuscript; E. Fuchs for the K14 expression cassette; and E. Koivunen, M. Helanterä, T. Tainola, and E. Rose for excellent technical assistance. Supported through the Finnish Cancer Organizations, the Finnish Academy, the Sigrid Juselius Foundation, the University of Helsinki, the State Technology Development Centre, and NIH.

22 January 1997; accepted 27 March 1997

Geometric Control of Cell Life and Death

Christopher S. Chen, Milan Mrksich, Sui Huang, George M. Whitesides, Donald E. Ingber*

Human and bovine capillary endothelial cells were switched from growth to apoptosis by using micropatterned substrates that contained extracellular matrix-coated adhesive islands of decreasing size to progressively restrict cell extension. Cell spreading also was varied while maintaining the total cell-matrix contact area constant by changing the spacing between multiple focal adhesion-sized islands. Cell shape was found to govern whether individual cells grow or die, regardless of the type of matrix protein or antibody to integrin used to mediate adhesion. Local geometric control of cell growth and viability may therefore represent a fundamental mechanism for developmental regulation within the tissue microenvironment.

The local differentials in cell growth and viability that drive morphogenesis in complex tissues, such as branching capillary networks (*1*, *2*), are controlled through modulation of cell binding to extracellular matrix (ECM) (*3*–*6*). Local disruption of ECM by pharmacologic or genetic means results in selective programmed cell death (apoptosis) within adjacent cells (*2*, *6*, *7*). Soluble integrin $\alpha_V\beta_3$ antagonists also induce apoptosis in cultured endothelial cells and promote capillary involution in vivo (*8*). Furthermore, death can be prevented by allowing suspended cells to attach to immobilized antibodies to integrins or by inhibiting tyrosine phosphatases (*7*, *9*). For these reasons, adhesion-dependent control of apoptosis has been assumed to be mediated by changes in integrin signaling. Analysis of capillary regression in vivo, however, has revealed that dying capillary cells remain in contact with ECM fragments, thus suggesting that the cell foreshortening caused by ECM dissolution may be the signal that initiates the death program (*2*). This possibility is supported by the finding that endothelial cells spread and grow on large (>100-μm diameter) microcarrier beads (*4*), whereas they rapidly die when bound to small (4.5 μm) ECM-coated beads (*10*) that cluster integrins and activate signaling but do not support cell extension (*11*).

Understanding how this apoptotic switch is controlled in capillary cells has enormous clinical implications, because angiogenesis is a prerequisite for tumor growth (*12*). Thus, we set out to determine whether cell shape or integrin binding per se governs life and death in these cells. We first measured apoptosis rates in suspended

C. S. Chen, S. Huang, D. E. Ingber, Departments of Surgery and Pathology, Children's Hospital–Harvard Medical School, Enders 1007, 300 Longwood Avenue, Boston, MA 02115, USA.
M. Mrksich and G. M. Whitesides, Department of Chemistry, Harvard University, Cambridge, MA 02138, USA.

*To whom correspondence should be addressed. E-mail: ingber@a1.tch.harvard.edu